POLITECNICO DI TORINO
Repository ISTITUZIONALE

Evaluation of LiDAR-Based Row Following Control for UAS Precision Spraying

Original
Evaluation of LiDAR-Based Row Following Control for UAS Precision Spraying / Nitti, L., Biglia, A., Sopegno, A., Messina, C., Grella, M., Malan, S., Gay, P., Comba, L.. - 586:(2025), pp. 680-687. (Biosystems Engineering Promoting Resilience to Climate Change - AIIA 2024 - Mid-Term Padova (Ita) 17-19 giugno 2024) [10.1007/978-3-031-84212-2_84].

Availability:
This version is available at: 11583/2999167 since: 2025-04-16T12:29:31Z

Publisher:
Springer Nature

Published
DOI:10.1007/978-3-031-84212-2_84

Terms of use:

This article is made available under terms and conditions as specified in the corresponding bibliographic description in the repository

Publisher copyright
Springer postprint/Author's Accepted Manuscript

This version of the article has been accepted for publication, after peer review (when applicable) and is subject to Springer Nature's AM terms of use, but is not the Version of Record and does not reflect post-acceptance improvements, or any corrections. The Version of Record is available online at: http://dx.doi.org/10.1007/978-3-031-84212-2_84

(Article begins on next page)

20 November 2026

Evaluation of LiDAR-based row following control for UAS precision spraying

Leonardo Nitti[1] [0009-0009-6711-2254], Alessandro Biglia[1] [0000-0002-4256-095X], Alessandro Sopegno[1] [0000-0002-6563-1052], Chiara Messina[1] [0000-0002-7504-8442], Marco Grella[1] [0000-0002-5932-8495], Stefano Malan[2] [0000-0002-5196-0402], Paolo Gay[1,*] [0000-0002-8342-425X] and Lorenzo Comba[1] [0000-0001-5466-0918]

[1] Department of Agricultural, Forest and Food Sciences, University of Turin
Largo Paolo Braccini 2 - 10095 Grugliasco (TO), ITALY
[2] Department of Electronics and Telecommunications (DET), Polytechnic of Turin
Corso Duca degli Abruzzi 24 - 10129 Torino (TO), ITALY
paolo.gay@unito.it

Abstract. In precision agriculture, automation is playing a key role in revolutionizing crop monitoring tasks and in-field operations. In this context, precision and spot spraying, performed by Unmanned Aerial Systems (UASs), are of great potential, allowing to save chemicals reducing drift, and modulating the spray in accordance with the real crop need. In addition, the UAS spraying can be performed when and/or where ground vehicles cannot be adopted.
In this work, the feasibility study of exploiting an on-board LiDAR based control system has been conducted, which allows UASs to precisely follow the vine row. In particular, a simulation tool has been developed to evaluate the relation between the altitude and pose of UAS and the LiDAR sensor Field Of View (FOV) within a detailed 3D model of vineyards. Moreover, the adoption of several LiDAR model can be simulated. The simulation tool was validated with real data from an experimental campaign held at DiSAFA vineyard in September 2023: (i) the accurate 3D model of the vineyard was generated by RGB imagery acquired with a DJI Mavic 2 Pro, and (ii) about 10,000 DJI Zenmuse L1 LiDAR frames have been acquired, using a DJI Matrice 350 RTK. Results proved that the LiDAR frame generated by the simulation tool are consistent with reference in-field acquired one.
The developed simulation tool enables the optimisation of the row following control system: indeed, different LiDAR models and mounting angles, and several vine row detection algorithms, can be tested avoiding expensive hardware implementation and in-field experiments.

Keywords: Prevision Viticulture, LiDAR, 3D Point Clouds, Flight control, Unmanned Aerial Vehicle.

1 Introduction

In precision agriculture, automation is playing a key role in revolutionizing crop monitoring tasks and in-field operations, both with aerial and ground uncrewed systems [1]. In this context, precision and spot spraying operations can benefit from the employment of UASs, allowing to save chemicals and modulating the spray according to the real need of the crop [2]. In addition, since these vehicles doesn't require an operator to work in the vicinity of the machine, the healthy risk of workers is thus reduced [3]. UAS spraying can be carried out in conditions otherwise unfavourable for ground vehicles (e.g. inaccessible terrains or with wet/slipping condition). However, in order to properly target the in-field operation on the crop, specific control strategies of UASs have to be developed, which allow, for instance, the UAS to accurately follow the vine row, flying at constant height over the top of the vine canopy [4].

In this context, LiDAR sensors demonstrated to be a valuable source of information regarding the environment in which the drones shall operate [5]. Indeed, LiDAR sensors provides 3D representations of the surface of the surrounding environment, by projecting laser beams at specific frequency and density over obstacles in the sensor field of view. However, this type of 3D data requires specific data processing methods to extract valuable information about the crop status and layout [6]. In particular, several vine row detection algorithms based on vineyard 3D models has been proposed [7]. Control systems to follow vine rows, based on on-board LiDARs, proved to be a viable and effective solution for precision agriculture Uncrewed Ground Vehicles (UGVs) [8]. However, in the UGVs application, the sensor is maintained at constant height relative to the ground during operations. On the contrary, for UASs applications, a wider set of altitudes and poses of the system can occur and hence, the possibility to exploit LiDAR based control strategies for UAS has to be investigated.

In this work, the feasibility of exploiting an on-board LiDAR based control system to allow UASs to properly follow the vine row, has been investigated. Specifically, a simulation tool has been developed to evaluate the effect of the UAS altitude and pose on the LiDAR sensor FOV in the vineyard environment. The developed simulation tool enables the optimisation of the row following control system: indeed, different LiDAR models and mounting angles, and several vine row detection algorithms, can be tested avoiding expensive hardware implementation and in-field experiments.

2 Simulation tool

In order to estimate the effect of the altitude and pose of an UAS on the LiDAR sensor Field Of View (FOV) in a vineyard environment, the developed simulator generates, as an output, a LiDAR frame (in the form of a 3D point cloud), given a set of inputs: (i) the UAS position and pose, (ii) the LiDAR model and (iii) its mounting angle on the UAS. In addition, an accurate 3D model of the agricultural environment within the simulated UAS is working is required, which should be in the form of a triangulated mesh. A simulated LiDAR frame is obtained by generating the set of LiDAR laser beams from the airborne sensor, and computing their impacts on the target surfaces (e.g. vine canopies or inter-row paths).

More in details, regarding the LiDAR sensor parameters, inputs of the tool are the FOV, the angular resolution and the maximum working distance. Moreover, the states of the sensor need to be given, namely the positions (in UTM coordinates with respect to the vineyard frame), angles (according to the RPY Euler convention), heights and displacements over the simulation time. Lastly, a mesh must be provided to determine the environment (e.g. the vineyard) in which the drone will operate.

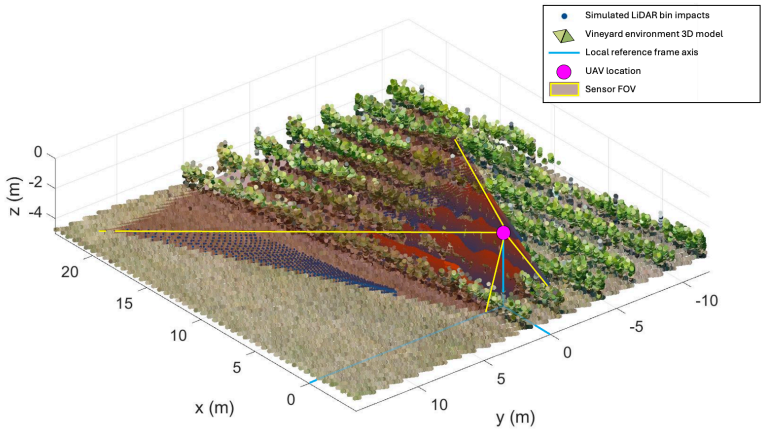


Figure 1. Graphical representation of simulation tool environment, with UAS position, a sample simulated LiDAR FOV (red) and the relative obtained LiDAR frame (blue dots), properly located within the 3D model of a vineyard

3 Validation

To validate the accuracy of the simulation tool, a comparison between simulated and real in-field acquired LiDAR frames has been performed. To accomplish that, an experimental campaign has been performed in a case study vineyard, located at Department of Agricultural, Forest and Food Sciences, University of Turin. The considered vineyard consists of 20 vine rows with a length of approximately 61 m each and it is characterized by a slope of 2°.

A set of more than 10000 frames has been recorded, accomplishing a series of flights with a DJI Matrice 350 RTK UAS, equipped with DJI Zenmuse L1 LiDAR (Fig. 2a). Each frame consists of a 3D point cloud of 1000 dots. During the acquisition phase, for each acquired LiDAR frame, the UAS flight parameters and pose (lat-lon position, altitude, roll-pitch-yaw angles) have been recorded, to be used as the simulation tool inputs.



(a) (b)

Figure 2. Picture of the case study UASs: (a) the DJI Matrice 350 RTK, equipped with DJI Zenmuse L1 LiDAR, and (b) the DJI Mavic Pro 2, equipped with high resolution RGB camera.

To generate the 3D mesh of the case study vineyard, an additional data acquisition phase was performed. Using the DJI Mavic Pro 2 UAS (Fig. 2b), a block of aerial RGB images of the case study vineyard has been acquired, and a high-density 3D point cloud model of the vineyard was generated with Agisoft Metashape structure from motion software. Finally, from the obtained 3D point cloud, the detailed 3D mesh of the environment has been generated via alpha shape method in MATLAB environment (Fig. 3), with the alpha value set at 0.97.

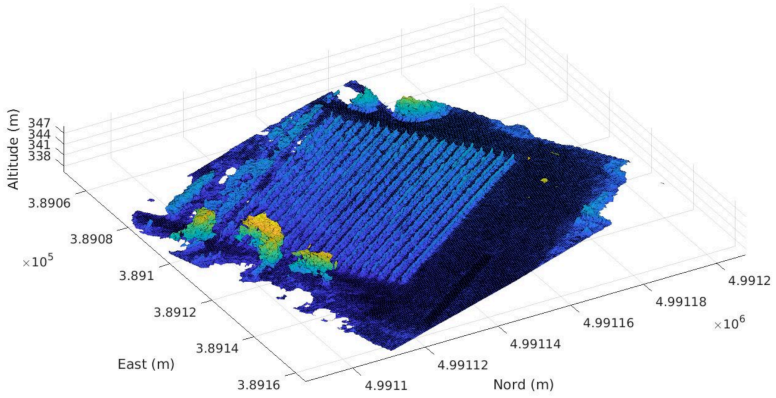


Figure 3. 3D triangulated mesh model of the DiSAFA case study vineyard, represented in the UTM 32N reference frame, generated for the validation phase of the simulation tool.

For each in-field recorded UAS position and pose, using the specific Zenmuse L1 sensor parameters and the 3D model of the case study vineyard, the simulated LiDAR frame has been generated.

The validation process involved a detailed comparison between each simulated and acquired LiDAR pairs of frames, to assess the quality and accuracy of the simulation tool. In this phase, the in-field acquired LiDAR frames are considered as reference ground truth. The comparison, performed with a quantitative approach, entailed the definition of a set of quality indices related to (1) the frame shapes and (2) the points (beam impacts) density distribution within the frame.

3.1 Frame shape error evaluation

The frame shape validation process aimed at verifying that the simulated sensors perceive the same portion of environment that the real one does (reference frame). This test is essential for the simulator validation since the length of the row that the sensor can see plays an important role in the performance of the row detection algorithm. The frame shape validation was performed on the horizonal plane, considering the projection of LiDAR points to the xy plane. Moreover, the convex hull enclosing the simulated and reference frame was computed, and two indices were defined, on the base of hulls area intersection. A graphical representation of a sample pair of simulated and reference LiDAR Zenmuse L1 frame is reported in Figure 3. The first quality index is the error one I_{err} (Eq. (1)), calculated as the difference between the simulated and the reference frame areas (namely $A_{acq}$and A_{sim}, respectively) enclosed by their hulls, normed with respect to A_{sim}. The second one is the overlapping index I_{ovlp} (Eq. (2)) which corresponds to the ratio between the intersection area A_{int}, as calculated in Eq. 3, and the a A_{acq}; the index reports if the two point clouds are seeing the same portion of environment. The higher the value of this parameter the better the simulation performed.

$$I_{err} = \frac{\left|A_{sim} - A_{acq}\right|}{A_{acq}} \tag{1}$$

$$I_{ovlp} = \frac{A_{int}}{A_{acq}} \tag{2}$$

$$A_{int} = A_{acq} \cap A_{sim} \tag{3}$$

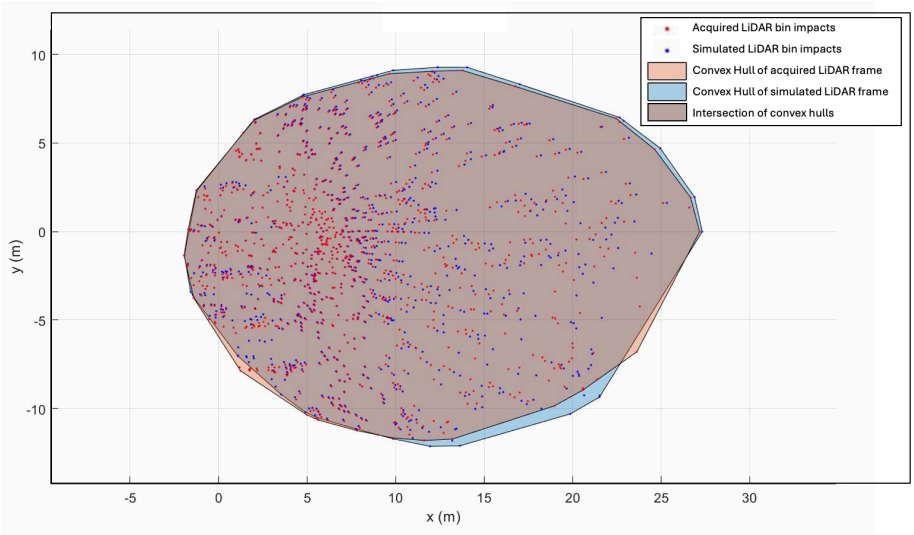


Figure 4. Projection on the xy plane of points belonging to two sample LiDAR frames: in-field acquired frame by DJI Zenmuse L2 LiDAR (red dots) and simulated one (blue dots), together with the computed convex hulls.

In addition, by approximating each convex hull to an ellipse, additional frame shape comparison can be performed, e.g. computing angle and length of the major and minor axis. In particular, three additional shape quality indices have been introduced, all defined as a difference between values obtained from the simulated and reference LiDAR frame: major axis angle difference and difference of major and minor axis length. For their computation, it is assumed that the points can be approximated with a Gaussian distribution with covariance Σ, which is a diagonalizable matrix. From the factorisation, it is possible to compute the ellipse that represents the level contour of the two-dimensional Gaussian, given a certain confidence interval. Since the eigenvalues λ_i are related to the length of the axis l_i, and the eigenvector represents the rotation matrix with an angle of α, the ellipse parameters of interest can be computed as reported in Eqs. (4) and (5).

$$l_i = \sqrt{\lambda_i} \tag{4}$$

$$\alpha = \cos^{-1}\left(U_{1,1}\right) \tag{5}$$

3.2 Points density distribution assessment

In addition to the shape analysis of the LiDAR frames, the validation of the simulation tools involved the investigation of the spatial distribution of points within each frame. Indeed, a different distribution of the points can lead to misleading information that can be extracted. To this aim, a voxelling phase was performed, dividing the plane into 10 cm squared elements, and computing an accumulation matrix, by counting the number of points located in each voxel. A graphical representation in false colour of the

accumulation matrix obtained processing a sample simulated and reference LiDAR frame is reported in Fig. 5. To compare each simulated frame with the respective in-field acquired reference one, the Pearson coefficient of correlation was adopted as index: high values in the Pearson coefficient indicates similarity between distributions.

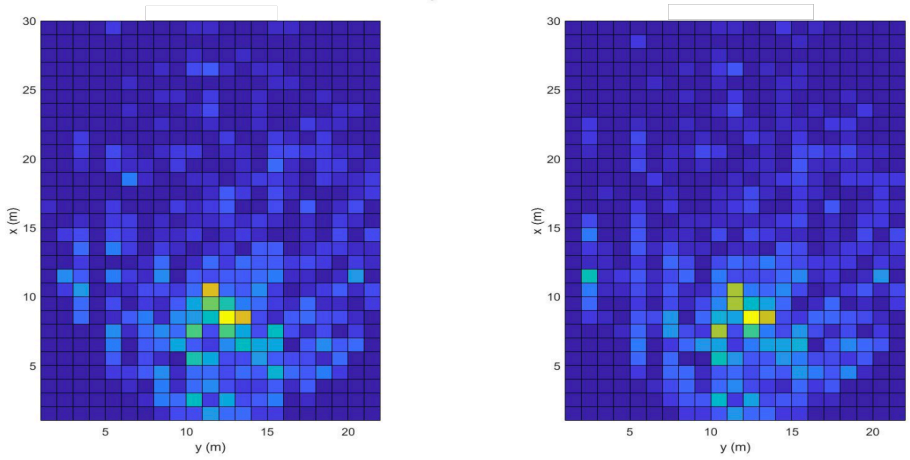


Figure 5. Graphical representation in false colour of the accumulation matrix obtained processing a sample simulated and reference LiDAR frame (blue=lower values, yellow=higher values).

4 Results and discussion

Values of defined frame quality indices, obtained by processing all the 10000 case study frames, are reported, in terms of average value and standard deviation, in Tab. 1. The average value of I_{ovlp} and I_{diff} indices, which are expressed as percentage, showed that, on average, each simulated frame properly represents more than the 95% of portion of vineyard environment represented in the simulated one. In addition, those quality indices expressed in meters, showed values generally lower than 0.3 meters, which are fully compatible with the here presented specific application. Finally, Pearson coefficient very close to 1 additionally proved the similarity between each simulate-reference frame pairs.

Table 1. Results of obtained quality indices for simulation tool validation

Parameter	Mean	Std. Deviation
I_{diff} (%)	3.21	1.83
I_{ovlp} (%)	95.70	1.45
Ellipse Major Axis Difference (m)	0.28	0.14
Ellipse Minor Axis Difference (m)	0.32	9.18
Ellipse Angle Difference (°)	1.17	1.17
Pearson Coefficient	0.85	0.04

5 Conclusions

In the context of assessing the feasibility of using LiDAR for UAS crop following task, a simulation tool to emulate the performances of a LiDAR sensor mounted on a UAS was developed, and validated to assess its accuracy with respect to the acquired data in a real case study vineyard. The developed simulation tool enables the optimisation of the row following control system: indeed, different LiDAR models and mounting angles, and several vine row detection algorithms, can be tested avoiding expensive hardware implementation and in-field experiments.

6 Fundings

This publication, is part of the project NODES which has received funding from the MUR – M4C2 1.5 of PNRR funded by the European Union - NextGenerationEU (Grant agreement no. ECS00000036)

7 References

1. Mammarella M, Comba L, Biglia A, Dabbene F, Gay P (2022) Cooperation of unmanned systems for agricultural applications: A theoretical framework. Biosystems Engineering 223(B):61-80. doi:10.1016/j.biosystemseng.2021.11.008
2. Biglia A, Grella M, Bloise N, Comba L, Mozzanini E, Sopegno A (2022) UAS- spray application in vineyards: Flight modes and spray system adjustment effects on canopy deposit, coverage, and off-target losses. Science of The Total Environment 845:157292. doi:10.1016/j.scitotenv.2022.157292
3. Yan X, Zhou Y, Liu X, Yang D, Yuan H (2021) Minimizing Occupational Exposure to Pesticide and Increasing Control Efficacy of Pests by Unmanned Aerial Vehicle Application on Cowpea. Applied Sciences 11(20):9579. doi:10.3390/app11209579
4. Mammarella M, Comba L, Biglia A, Dabbene F, Gay P (2022) Cooperation of unmanned systems for agricultural applications: A case study in a vineyard. Biosystems engineering 223(B):81-102. doi:10.1016/j.biosystemseng.2021.12.010
5. Rivera G, Porras R, Florencia R, Sánchez-Solís JP (2023) LiDAR applications in precision agriculture for cultivating crops: A review of recent advances. Computers and Electronics in Agriculture 207:107737. doi:10.1016/j.compag.2023.107737
6. Comba L, Zaman S, Biglia A, Ricauda Aimonino D, Dabbene F, Gay P (2020) Semantic interpretation and complexity reduction of 3D point clouds of vineyards. Biosystems Engineering 197:216-230. doi:10.1016/j.biosystemseng.2020.05.013
7. Biglia A, Zaman S, Ricauda Aimonino D, Gay P, Comba L (2022) 3D point cloud density-based segmentation for vine rows detection and localization. Computers and Electronics in Agriculture 199:107166. doi:10.1016/j.compag.2022.107166
8. Nehme H, Aubry C, Solatges T, Savatier X, Rossi R, Boutteau R (2021) LiDAR-based structure tracking for agricultural robots: Application to autonomous navigation in vineyards. Journal of intelligent & robotic systems 103(4):61. doi:10.1007/s10846-021-01519-7.